Mechanical Behavior of a Tightly Woven Carbon-Carbon Composite

A. Ozturk
Metallurgical Engineering Department, Middle East Technical University
Ankara 06531, Turkey

ABSTRACT

The mechanical properties and failure behavior of a tightly woven carbon-carbon composite were investigated and correlated with microstructural features. The analysis of fracture surfaces and microstructural characterization were accomplished using scanning electron microscopy. The tensile strength, flexural strength, fracture toughness, and failure mechanisms of this composite were determined at elevated temperatures. Strength and fracture toughness of the composite increased in argon, but decreased in air as the temperature increased. Microscopic observations of the fracture surfaces of the broken specimens revealed that the composite failed in a tension/shear mixed mode rather than in pure tension.

1. INTRODUCTION

Carbon fiber reinforced carbon matrix composites (carbon-carbon composites) are of great importance since they possess a variety of unique engineering properties /1-3/. These composites offer better thermal /4/, mechanical /4-6/ and fracture mechanics /7,8/ properties when compared with the properties of ceramics and super alloys. The major advantage of the carbon-carbon composites for high temperature applications is that they retain their high specific strength and elastic modulus at elevated temperatures in inert atmospheres /2,9/. Because of these superior thermal and mechanical properties which persist at high temperatures, carbon-carbon composites find special uses as structural materials in aeronautic and space industries /1-3/. Applications such as exit nozzles for rockets, nose caps and leading edges for missiles and space shuttles, nuclear reactors and especially for fusion devices have been reported in the literature. Newer applications, such as hot press dies, wind tunnel models, racing car components, commercial disc brakes and sporting goods, etc., are being developed /10/.

Evaluation of the thermal and mechanical properties of these composites is essential if they are to be utilized for structural applications. The desired properties in various applications may be obtained by controlling the microstructure of the matrix /11,12/, the selection of fiber /13,14/ and the type of weaving /15/. Moreover, the interface between fiber and matrix is one of the important factors which influences the fracture behavior and hence the ultimate mechanical properties /7,8/.

In spite of some investigations on the development, properties and fracture behavior of carbon-carbon composites, the data are sparse compared with ceramics and super alloys. Studies on the mechanical properties of these composites have remained an area of research relatively uncommunicated to the open literature. Results have been kept secret due to the defense related applications. Therefore, any contribution in this field will be an asset for related industries. A good understanding of the mechanics of these composites is necessary if they are to be used in applications requiring high strength and high toughness.

The purpose of this investigation was to determine

the strengths and fracture toughness of a tightly woven carbon-carbon composite at ambient and elevated temperatures. Mechanical testing was supplemented with microstructural characterization to provide information necessary to explain observed behavior. The fracture surfaces of the composite were examined to locate fracture sources and to study the fracture propagation patterns.

2. EXPERIMENTAL

A. Specimen Preparation

The carbon-carbon composite used in this study was a commercial material (K-Karb) obtained in panel form from Kaiser Aerotech Company, San Leandro, CA, USA. The composite consists of graphite fiber reinforced graphite matrix developed for aerospace applications. The fiber reinforcement was in a plain weave woven fabric form. Readers are referred to references 5 and 16 for details of the fabrication of these composites.

Test specimens were prepared by cutting the composite panel into small rectangular bars along the warp (length) direction using a diamond saw. The nominal dimensions of these bars were 101.6 by 7.6 by 6.3 mm. The thickness of the bars was ground to approximately 5.0 mm to obtain a larger span to depth ratio during flexural testing. Grinding was accomplished using 600 grit silicon carbide grinding papers. The nominal dimensions of flexural test specimens were 101.6 by 7.6 by 5.0 mm. A typical flexural test specimen geometry is shown in Fig. 1a.

Static tensile test specimens were prepared by machining the as cut rectangular-shaped composite bars with a surface grinder. A 220 grit diamond wheel was used to reduce the gauge section. The length and the width of the parallel-sided gauge section were approximately 25.4 and 5.0 mm, respectively. A typical uniaxial tensile test specimen geometry is shown in Fig. 1b. Finally a glued-on strain gauge, supplied by MTS Measurement Group Inc., was mounted on the specimen to measure the strain to failure.

Specimens were produced for toughness tests in much the same way as those for the flexure tests. However, due to the lack of quantity of the specimens, the rectangular bars were cut into two pieces to increase the number of specimens. Also, the width and the thickness of the specimens were ground to approximately 5.0 mm using 600 grit silicon carbide grinding papers. The nominal dimensions of the toughness specimens were 50.8 by 5.0 by 5.0 mm. Specimens were notched in the center using a diamond blade with a thickness of 0.3 mm and were assumed to include micro cracks at the tip of the notch due to machining.

B. Testing

Flexural strength tests were conducted in three-point bending employing a Satec model UTC6OHVL com-

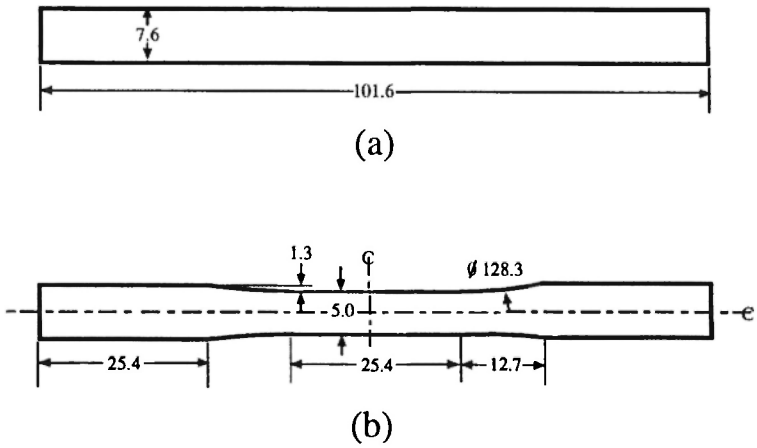

Fig. 1: Schematic illustration of test specimens. (All dimensions in mm.)

pression/tension mechanical test unit. Three-point bending tests were performed at room temperature, 500 and 800 °C in air and in argon. The temperature was measured using a K-type thermocouple. For each test condition, specimens were brought up to the temperature and broken one after another once the temperature was stabilized.

The crosshead displacement rate was maintained at 0.5 mm/min for all flexural tests. The span length to specimen depth ratio (S/d) was 10, which was not large enough to impede a shear failure in the çomposite. The modulus of rupture (MOR) was calculated based on the assumption that the composite behave elastically until the maximum tensile stress is achieved.

Static tension tests were performed under ambient laboratory conditions using a servo hydraulic testing machine (MTS Model 810). A double set of universal joints were used to eliminate possible misalignment and to ensure a homogeneous state-of-strain over a uniform gauge section. Once the test assembly was set up, a tension load was applied to the specimen at a constant loading rate of 18.1 kg/min. The stress at the maximum load applied to the specimen was taken as the ultimate tensile strength. Specimen failure was taken as the point at which specimen fractured into two pieces.

Values for fracture toughness were calculated using the ASTM single edge notched bend test. The testing procedure was similar to the testing procedure for three-point bend strength testing. However, the S/d ratio was 5 for toughness tests.

C. Microstructure Analysis

The fracture surfaces of broken specimens were examined in a JOEOL JSM-T330A scanning electron microscope in order to determine the fracture mechanisms leading to the final fracture of the composite. Specimens for fractographic analysis were prepared by cutting fracture end from the bar. No coating was necessary for the specimen to be analyzed.

3. RESULTS AND DISCUSSION

A. Flexural Strength

In order to gain statistical accuracy, three specimens were tested for a single experimental condition. The ultimate flexural strength was calculated for all specimens based on maximum loads and the initial dimensions of the specimens. All values were retained in computing the averages. The validity of the averages was confirmed by a randomization test (t-test) at a 95% confidence level with respect to the probability points of the two sided reference distribution /17/. The maximum uncertainty in measurements was calculated using error analysis as ± 1 MPa.

The values of flexural strength are reproducible to within ± 6.4, ± 5.3 and ± 8.0 MPa in air and ± 5.9, ± 3.9 and 3.8 MPa in argon at room temperature, 500 and 800 °C, respectively. The plus and minus signs indicate ± 1 standard deviation from the averages. The corresponding percentages of the reproducibility of each set of tests are approximately 5, 4 and 28 % in air and 4, 3 and 3 % in argon, respectively. The resultant data indicate that the reproducibility of the average values are very good except for data taken at 800°C in air when extensive specimen oxidation occurred during testing. The high reproducibility of the averages is attributed to the weave pattern of the reinforcing fibers and hence the uniform distribution of the stresses between fibers in the warp and fill direction. Manocha and Bahl /15/ concluded that distribution of load among the reinforcing fibers in woven fabric carbon-carbon composites is improved due to the better orientation of the fiber tows. The poor reproducibility of the tests conducted at 800°C in air is due to the testing time-at-temperature. It was consistently observed in this study that the specimen which was exposed for longer time at temperature had more deterioration than the previous specimens tested at the same temperature. Consequently, composites exhibit lower strength due to the severe oxidation of the matrix and fibers, and hence resultant brittleness.

The effect of temperature on the flexural strength of the composite is different in air and argon. The variation of flexural strength in air and in argon is plotted as a function of temperature in Fig. 2. The error bands indicate the ± 1 standard deviation limits of the determination. As seen in Fig. 2, MOR increases slightly with increasing temperature in argon, but decreases in air as the temperature increases. The results of flexural tests agree with the results reported

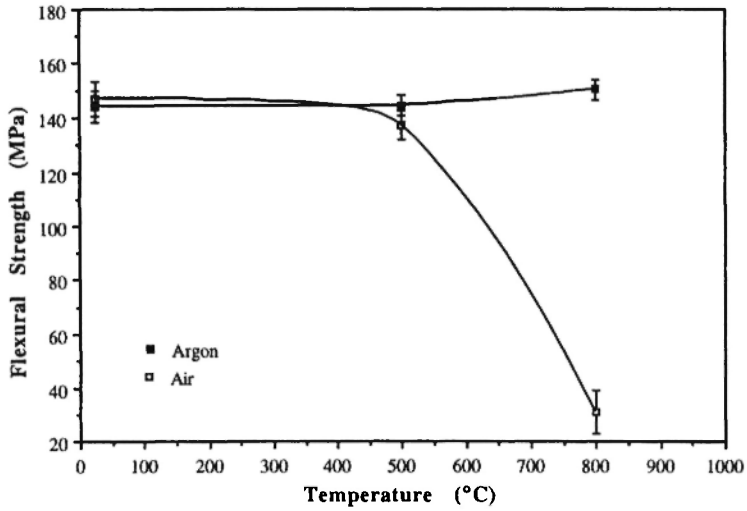

Fig. 2: Variation in flexural strength as a function of temperature.

for pitch and PAN carbon felt composites by Sato *et al.* /4/. The reason for the increase in strength with increasing temperature is that the strong covalent bonding of carbon produces low carbon atom diflusivities. On the other hand, the decrease in flexural strength with increasing temperature is attributed to the oxidation of the composite. It has been reported /9/ that oxidation of carbon-carbon composites starts at temperatures as low as 500°C in air, and the rate of oxidation increases as the temperature increases. This behavior was also observed in this study.

The average ultimate flexural strength (AUFS) of the composite based on the three specimens is 147.1 ± 6.4 MPa in air at room temperature. Some load bearing capability was retained beyond the ultimate strength because the shear characteristics of the composite caused the crack to deflect along the interface between layers. Flexural strength of this composite at room temperature is more than five times greater than flexural strength of a fine grained isostatically pressed graphite (IG-11) whose value for the flexural strength was reported as 39.6 MPa at room temperature /4/. The resultant data indicate that the flexural strength of the graphite matrix of the composite is improved with the incorporation of carbon fibers.

It appears that an increase in temperature up to 500°C in argon did not have a significant effect on the flexural strength of this composite. However, the AUFS increased from 144.3 ± 3.9 MPa to 150.4 ± 3.8 MPa when the temperature increased from 500°C to 800°C in argon. Under oxidizing conditions the AUFS decreased slightly when the temperature was raised to 500°C in air. Further increase in temperature beyond 500°C resulted in a significant decrease in strength. The AUFS decreased from 137.2 ± 5.3 MPa to 31.0 ± 8.0 MPa as the temperature increased from 500°C to 800°C in air.

In order to measure the flexural strength of the composite panel in the fill (width) direction, three specimens were tested at room temperature in air. The AUFS of the three specimens broken in the fill direction, 146.3 ± 5.3 MPa, were almost the same as that in the warp direction. This indicates that the applied load was uniformly distributed among the reinforcing fibers in both the warp and fill directions.

The representative load versus crosshead displacement curves for this composite tested in three-point bending at room temperature and 800°C are depicted in Fig. 3. For the tests conducted at room temperature and at 500°C, the load increased linearly with increasing displacement up to a maximum and then a substantial abrupt load drop (~ 1/3 of the maximum load) was followed by a stepwise decrease of the load. Similar curves have been reported for carbon-carbon composites by Oh and Lee /7/, for carbon fiber reinforced glass ceramic composites by Sambell *et al.* /18/ and for SiC fiber reinforced glass ceramic composites by Prewo and Brennan /19/ and Marshall and Evans /20/.

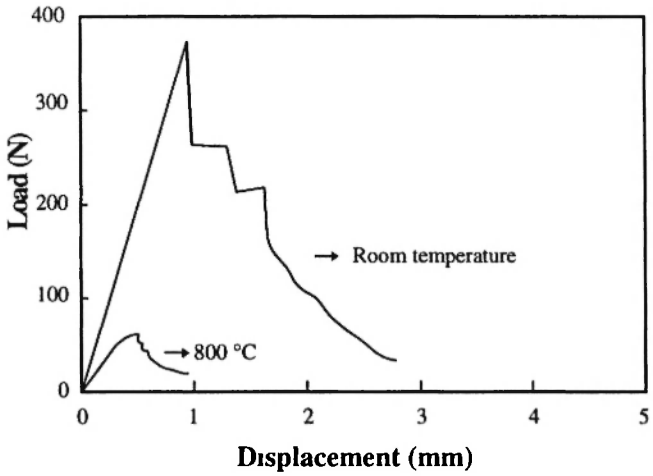

Fig. 3: Typical load-displacement curves for flexural strength tests in air.

Although the AUFS decreased, the general appearance of the load-displacement curves of the specimens tested in air at 500°C were similar to those of the specimens tested at room temperature. However, specimens tested at 800°C showed a somewhat different behavior. Load-displacement curves exhibited a linear behavior up to a discontinuity. Beyond this point load increased nonlinearly, reached a maximum, and then dropped in a stepwise manner as seen in Fig. 3. Direct observation of the test specimen after the test revealed that the composite experienced severe oxidation during testing. As was evident from the appearance of the specimen, the high temperature degradation of this composite involves chemical oxidation effects associated with the air environment.

The load-displacement curves of the specimens tested in argon at room temperature, 500°C and 800°C were almost the same as the curves of the specimens tested at room temperature and at 500°C in air.

The SEM analysis of the specimens broken in flexure revealed two types of failure behavior: crack propagation perpendicular to the plane of the cloth layer and delamination of the cloth layers (see Fig. 4). The failure initiated on the tensile surface of the specimen and proceeded through the specimen thickness with cracks propagating in a delamination mode. These observations indicate that the composite failed in a tension/shear mode rather than in pure tension. This is due to the low span-to-depth ratio which may induce the interlaminar shear failure or mixed failure of the composite. Another reason for the mixed failure is attributed to the weak fiber-matrix bond which impedes crack deflection and branching at the fiber-matrix interface /7,8/. It is known that weak fiber-matrix interface serves to arrest cracks, resulting in splitting of the advancing crack. As a result, high strength and a pseudo-plastic fracture pattern may be achieved even if the matrix is brittle /13/.

Figure 5 is a SEM fractograph of the broken surface

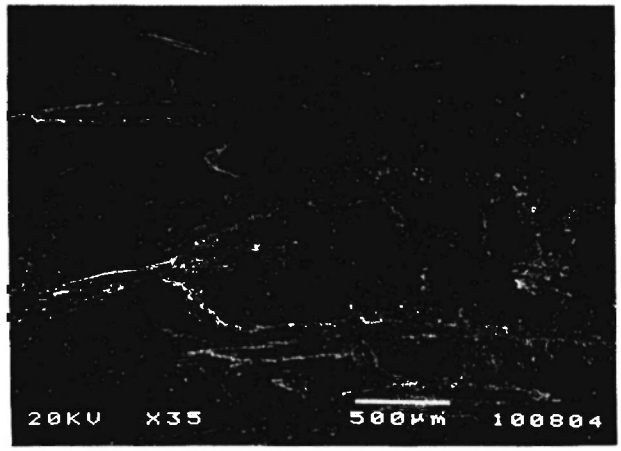

Fig. 4: SEM micrograph of a carbon-carbon composite specimen broken in flexure showing crack branching and delamination. (Bar = 500 µm.)

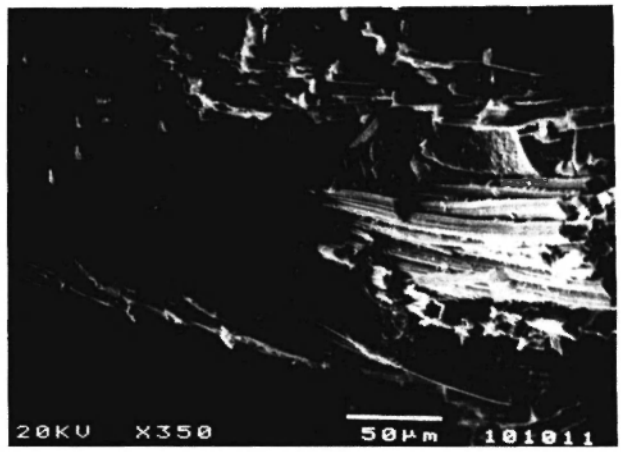

Fig. 5: SEM fractograph of a carbon-carbon composite specimen broken in flexure showing the separation of matrices, fiber bridging and fiber pull-out. (Bar = 50 µm.)

of a flexural test specimen showing pull-out of fibers from the matrix, debonding of fiber-matrix interfaces, and separation of matrices. Radial and circumferential microcracks are observed in the matrix, and are shown in Fig. 6. In general, these cracks are observed to propagate through regions of closely spaced fibers. The critical stress for the formation of matrix cracking has been evaluated by Aveston *et al.* /21/ who reported that the matrix cracks represent extensive damage to the matrix. Davidge /22/ has reported that because of the stress enhancement effect in the fibers, the most likely origin of the fiber failure is near to a matrix crack. In this study, fiber failure is observed to initiate near to a matrix crack. Observations are in good agreement with Davidge's findings.

B. Tensile Strength

Five specimens were broken in tension to determine the average ultimate tensile strength (AUTS) of the composite panel. The ultimate tensile strength was calculated for all five specimens based on maximum loads and the initial dimensions of the specimens. All values were retained in computing the averages since only five data points were available. The t-test was applied to determine the validity of the average. However, the uncertainties of the data for the individual tensile test were calculated using error analysis as ± 0.1 MPa, ± 0.01 GPa and ± 0.01% for the tensile strength, the elastic modulus and the failure strain, respectively. Results of uniaxial tensile tests are presented in Table 1 along with the average, the ± 1 standard deviation and the variance. The AUTS, 92.1 ± 3.7 MPa, of this composite panel was different from the AUTS's (104.8 ± 5.2 and 62.3 ± 3.9 MPa) of the panels reported elsewhere /5,16/. Fiber failure is observed to initiate near to a matrix crack. It was not determined why the strength values differed from panel to panel; however, the same stress-strain behavior was observed for all the composite panels during static tensile testing. The initial strength of specimens broken in tension ranged from 88.1 ± 0.1 MPa to 97.5 ± 0.1 MPa. Failure was catastrophic and occurred in the gauge section. All specimens failed in a fibrous mode with some shear parallel to the fibers in the warp direction.

The resultant data indicate that the composite has lower strength in tension than in bending. The AUTS is 92.1 ± 3.7 MPa but the AUFS is 147.1 ± 6.4 MPa. Similar results have been obtained for SiC fiber reinforced glass ceramic composites where it was suggested that the strength difference in the two tests may be due partly to flawed statistics /19/. Moreover, it has been reported that once the first crack forms in flexural testing, the uniformity of the beam is destroyed and the stresses in the beam are no longer related solely to the applied load and specimen dimension /19/.

Fractographs obtained from the specimens which

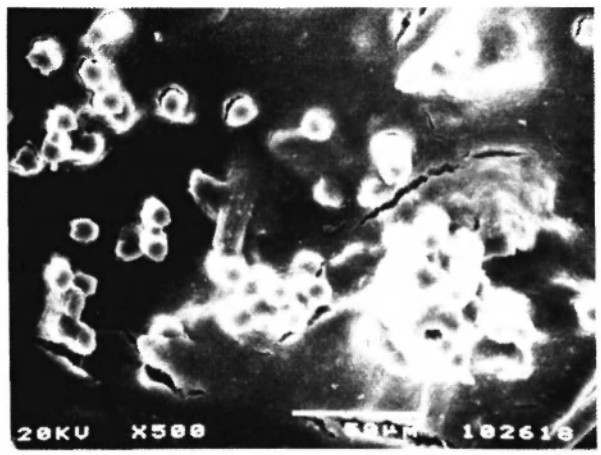

Fig. 6: SEM fractograph of a carbon-carbon composite specimen broken in flexure showing radial and circumferential cracks in the matrix. (Bar = 50 μm.)

Table 1
Static tensile properties of the carbon-carbon composite

	Tensile strength (MPa±0.1)	Elastic modulus (GPa±0.01)	Failure strain (% ± 0.01)
	97.5	----	----
	92.9	9.03	1.03
	88.1	8.98	0.98
	89.3	----	----
	92.7	----	----
Average	92.1	9.01	1.01
Standard dev.	3.7		
Variance	13.5		

were static tensile tested suggested that the microstructure of these specimens was similar to the microstructure of the flexure tested specimens. A representative fractograph of a static tensile tested specimen illustrates fiber pull-outs and cracks extending around the fibers and into the matrix (see Fig. 7).

C. Fracture Toughness

The fracture toughness, as expressed by the critical stress intensity factor, K_{Ic}, of this composite was measured at room temperature, 500°C and 800°C in air and in argon. Three specimens were tested during a single experiment to determine the numerical values for K_{Ic}. All data points were retained in computing the averages of K_{Ic} since only three values were available for each set of tests.

The variation of plane strain fracture toughness, K_{Ic}, is plotted as a function of temperature in air and argon in Fig. 8. The error bands indicate ± 1 standard deviation limits of the determinations. A comparison of Figs. 2 and 8 reveals that results resemble those for the flexural strengths. As seen in Fig. 8. K_{Ic} decreases with increasing temperature in air, but remains almost the same in argon.

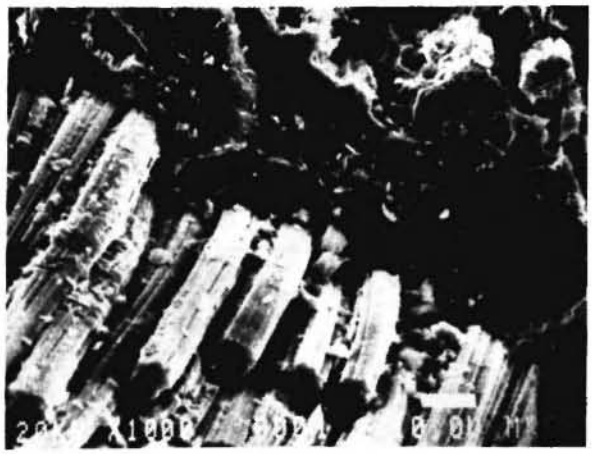

Fig. 7: SEM fractograph of a carbon-carbon composite specimen broken in tension showing fiber pull-out and cracks propagating around the fibers and into the matrix. (Bar = 10 μm.)

Similar results have been observed for pitch and pan fiber felt composites by Sato *et al.* /4/. The reasons for the variation in K_{Ic} with increasing temperature are probably the same as those for flexure tests. The values for K_{Ic} in air and in argon are about the same, 4.4 ± 0.2 MPa.m$^{1/2}$ and 4.5 ± 0.2 MPa.m$^{1/2}$, respectively, at room temperature. It has been reported that hot pressed Norton Co. NC-132 Si_3N_4, one of the toughest monolithic ceramics, possesses a K_{Ic} of 4.5 MPa.m$^{1/2}$ at room temperature /23/. A fine grained isostatically pressed graphite (IG-11) has been reported to exhibit a K_{Ic} of about 0.8 MPa.m$^{1/2}$ at room temperature /4/. Consequently, this composite exhibits a fracture toughness better than or equal to the fracture toughness of monolithic ceramics and fracture toughness of the graphite matrix of the composite was improved when carbon fibers are incorporated.

The values of K_{Ic} are the same, 4.5 ± 0.2 MPa.m$^{1/2}$, at 500°C and 800°C in argon. However, a significant decrease in K_{Ic} was obtained when the temperature was raised from 500°C to 800°C in air. The corresponding values of K_{Ic} were 4.20 ± 0.3 MPa.m$^{1/2}$ and 1.1 ± 0.3 MPa.m$^{1/2}$, respectively. The decrease in K_{Ic} at elevated temperatures in air is attributed primarily to the severe oxidation of the specimen during testing.

Fracture toughness of the composite was also measured in the fill direction at room temperature in air. The average value of K_{Ic} in the fill direction, 4.3 ± 0.2 MPa.m$^{1/2}$, reveals that the composite fracture toughness was almost the same in the warp and fill directions.

The representative load versus displacement curves of the fracture toughness tests in air at room temperature and 800°C are depicted in Fig. 9. The curves closely resemble the flexural strength curves. The load to failure increased linearly at room temperature and 500°C both in air and in argon. However, the specimens tested at 800°C in air exhibited a nonlinear behavior in the load-displacement curve. After reaching a maximum, a stepwise load drop occurred for all specimens at all temperatures. None of the specimens failed completely. They remained in one piece, still capable of carrying a substantial load. The cracks propagating from the notch tip never reached the compression side of the specimens. The micrographs in Fig. 10 show the propagation of a crack from the notch

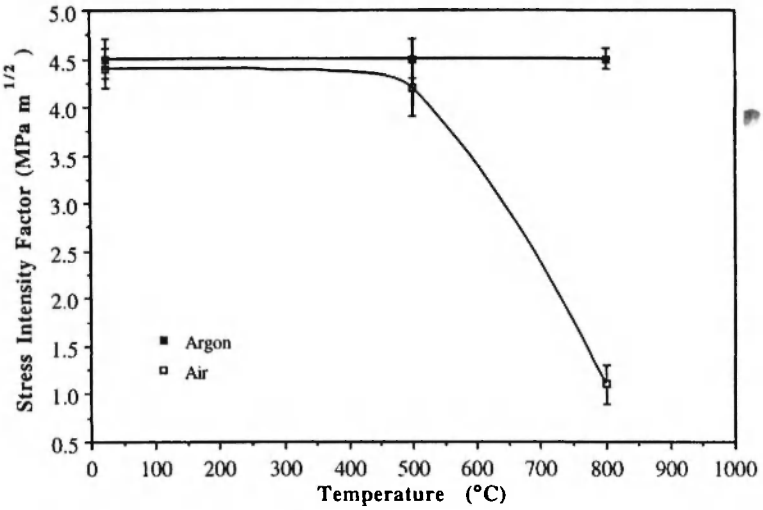

Fig. 8: Variation in the composite fracture toughness as a function of temperature.

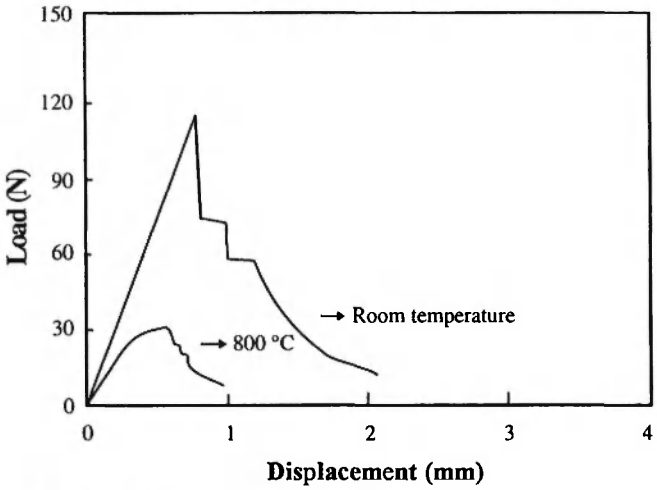

Fig. 9: Typical load-displacement curves of fracture toughness tests in air.

tip. The micrograph in Fig. 10a was obtained just after achievement of the maximum load. Figure 10b is the micrograph of the same specimen after the maximum load and a substantial amount of displacement are achieved. The micrographs clearly show that the specimens exhibited multiple matrix cracking, fiber pull-out, crack branching, and deflection between layers, during loading.

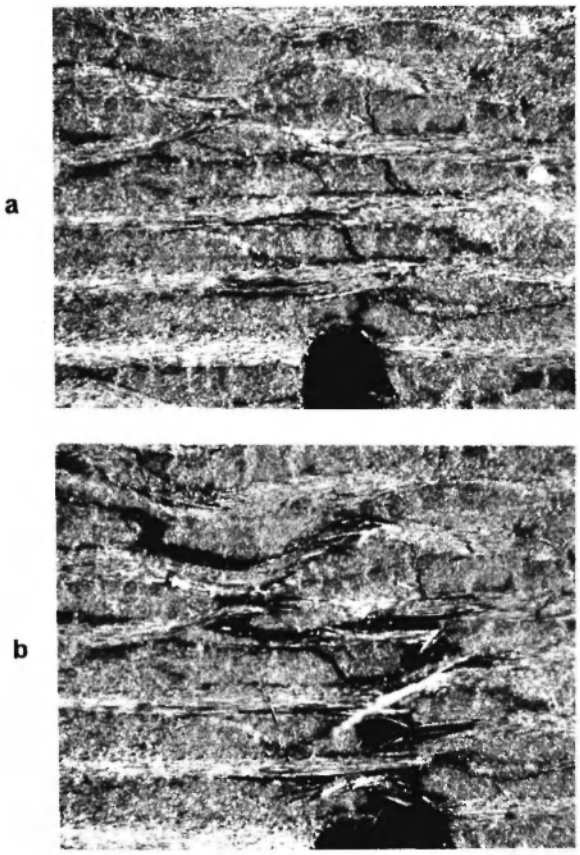

Fig. 10: Micrographs of a fracture toughness test specimen showing the crack propagating from the notch tip. (40×)

4. CONCLUSIONS

An investigation of the strength and toughness of a tightly woven carbon-carbon composite has led to the following conclusions:

1. The composite investigated has a weak bond strength between the fibers and the matrix. It exhibits extensive fiber pull-out and hence improved mechanical performance.
2. The composite exhibits high bend and tensile strength at ambient temperatures. It maintains its strength at elevated temperatures in an inert atmosphere. However, bend and tensile strengths of the composite decrease significantly at elevated temperatures in an oxidizing atmosphere. The high temperature degradation of the composite is attributed to chemical oxidation effects associated with the air environment.
3. The fracture toughness of the composite decreases as temperature increases in air, but it remains the same in argon.
4. Matrix cracking, fiber failure, pull-out of individual fibers and fiber bundles, fiber debonding, and crack branching are the dominating toughening mechanisms in this composite.

ACKNOWLEDGEMENTS

The author is grateful to Kaiser Aerotech Company, San Leandro, California, USA, for providing the composite panel. He would like to thank Dr. Robert E. Moore and Dr. Jowoong Ha for their help, comments and valuable discussions.

REFERENCES

1. E. Fitzer. The future of carbon-carbon composites, *Carbon*, **25**, 163-190 (1987).
2. J.D. Buckley. Carbon-carbon, an overview. *Am. Ceram. Soc. Bull.*, **67**, 364-368 (1988).
3. A.A. Baker. High performance fibre composites for aircraft applications: An overview. *Met. Forum*, **6**, 81-101 (1983).
4. S. Sato, A. Kurumada, H. Iwaki and Y. Komatsu. Tensile properties and fracture toughness of carbon-fiber felt reinforced carbon composites at high temperature. *Carbon*, **27**, 791-801 (1989).
5. A. Ozturk and R.M. Moore. Tensile fatigue behaviour of tightly woven carbon-carbon composites, *Composites*, **23**, 39-46 (1992).
6. L.M. Manocha, O.P. Bahl and Y.K. Singh. Mechanical behavior of carbon-carbon composites made with surface treated carbon fibers, *Carbon*, **27**, 381-387 (1989).
7. S.-M. Oh and J.-Y. Lee. Fracture behavior of two-dimensional carbon/carbon composites, *Carbon*, **27**, 423-430 (1989).
8. K.Y. Sohn, S.-M. Oh and J.-Y. Lee. Failure behavior of carbon-carbon composites prepared by chemical vapor deposition, *Carbon*, **26**, 157-162 (1988).
9. D.W. Mckee. Oxidation behavior and protection of carbon/carbon composites, *Carbon*, **4**, 551-557 (1987).
10. K.K. Chawla. *Composite Materials Science and Engineering*, Springer-Verlag, New York, 1987; pp. 150-163.
11. S.-M. Oh and J.-Y. Lee. Effects of matrix structure on mechanical properties of carbon/carbon composites, *Carbon*, **26**, 769-776 (1988).
12. E. Yasuda, Y. Tanabe, L.M. Manocha and S. Kimura. Matrix modification by graphite powder additives in carbon fiber/carbon composite with thermosetting resin precursor as a matrix, *Carbon*, **26**, 225-227 (1988).
13. L.M. Manocha, E. Yasuda, Y. Tanabe and S. Kimura. Effect of carbon fiber surface-treatment on mechanical properties of C/C composites, *Carbon*, **26**, 333-337 (1988).
14. E. Fitzer, K.-H. Geigl and W. Huttner. The influence of carbon fibre surface treatment on the mechanical properties of carbon/carbon composites, *Carbon*, **18**, 265-270 (1980).
15. L.M. Manocha and O.P. Bahl. Influence of carbon fiber type and wave pattern on the development of 2D carbon-carbon composites, *Carbon*, **26**, 13-21 (1988).
16. Technical report on K-Karb composite, Kaiser Aerotech Company, San Leandro, California, USA.

17. G.E.P. Box, W.G. Hunter and J.S. Hunter. *Statistics for Experimenters,* John Wiley and Sons, New York, 1978; pp. 93-105.
18. R.A.J. Sambell, A. Briggs, D.C. Phillips and D.H. Bowen. Carbon fiber composites with ceramic and glass matrices, Part 2 - Continuous fibers, *J. Mater. Sci.*, 7, 676-681 (1972).
19. K.M. Prewo and J.J. Brennan. High-strength silicon carbide fibre-reinforced glass-matrix composites, *J. Mater. Sci.*, **15**, 463-468 (1980).
20. D.B. Marshall and A.G. Evans. Failure mechanisms in ceramic-fiber/ceramic-matrix composites, *J. Am. Ceram. Soc.*, **68**, 225-231 (1985).
21. J. Aveston, G.A. Cooper and A. Kelly. Single and multiple fracture, in: *The Properties of Fiber Composites,* Conference proceedings of the national physical laboratory, IPC Science and Technology Press Ltd., Surrey, England, 1971; pp. 15-26.
22. R.W. Davidge. *Mechanical Behaviour of Ceramics,* Cambridge University Press, 1979; pp. 104-117.
23. O. Sbaizero and A.G. Evans. Tensile and shear properties of laminated ceramic matrix composites, *J. Am. Ceram. Soc.*, **69**, 481-486 (1986).